Khalili *et al. Biochar* (2024) 6:6
https://doi.org/10.1007/s42773-023-00286-y

Biochar

ORIGINAL RESEARCH Open Access

Biochar: a high performance and renewable basic carbocatalyst for facilitating room temperature synthesis of 4*H*-benzo[*h*]chromene and pyranopyrazoles in water

Dariush Khalili[1*], Ali Asghar Ramjerdi[1], Hamid Reza Boostani[2] and Arash Ghaderi[3]

Abstract

This study has introduced a pioneering methodology by employing biochars as a basic carbocatalyst in the context of multicomponent reactions. Biochars were produced from different manures and organic wastes using the pyrolysis-carbonization process under limited oxygen conditions. The prepared biochars were well characterized using Fourier transform infrared spectroscopy (FT-IR), scanning electron microscopy (SEM), energy-dispersive X-ray spectroscopy (EDX), Brunauer–Emmett–Teller (BET) analysis, and powder X-ray diffraction (XRD). The chemical characteristics and potentiometric titration analysis provide compelling evidence of the intriguing basicity properties exhibited by the prepared biochars. The pH values, ash content, and potentiometric titration results confirmed the exceptional basicity characteristics of cow manure biochar formed at 600 °C (CB600), establishing it as the most basic carbocatalyst in this study. Encouraged by these initial results, the activity of the biochars as basic carbocatalysts was evaluated in multicomponent synthesis of 4*H*-benzo[h]chromene and pyranopyrazoles and 600 °C exhibited the most pronounced catalytic performance owing to its superior total basicity. By these findings, it can be asserted that this work introduces the groundbreaking application of biochars as potent basic carbocatalysts for the multicomponent synthesis of structurally diverse heterocycles. Unveiling the vital basic role of biochars will definitely open up new opportunities in organic chemistry and provide salient features for environmentally-friendly chemistry, including easy retrieval, non-toxicity, and widespread accessibility.

Highlights

- Biochars were introduced as potent basic carbocatalysts for multicomponent synthesis of heterocycles.
- Quantitatively assess basicity of the prepared biochars was performed using potentiometric titration.
- The activity of the biochars as basic carbocatalysts was evaluated in multicomponent synthesis of chromenes and pyranopyrazoles.

Keywords Biomass, Biochar, Basic carbocatalyst, Heterogeneous catalysis, Multicomponent synthesis, Environment sustainability

Handling editor: Hailong Wang.

*Correspondence:
Dariush Khalili
khalili@shirazu.ac.ir
Full list of author information is available at the end of the article

Graphical Abstract

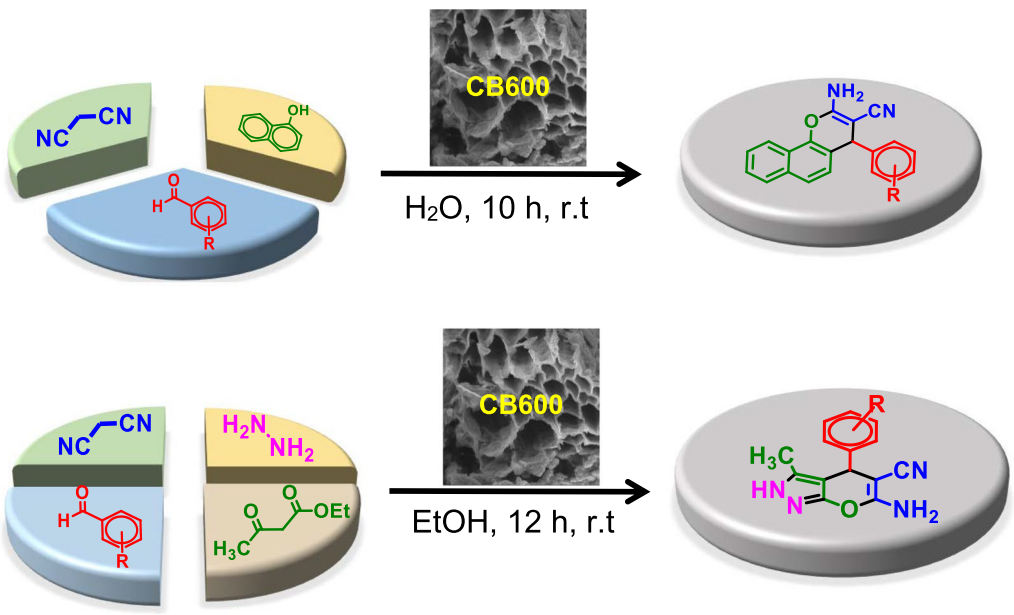

1 Introduction

In order to ensure a sustainable future for both society and the scientific community, we must prioritize the use of renewable feedstocks, mainly due to the escalating concerns pertaining to environmental pollution and the growing severity of energy shortages (Albers et al. 2016). Biomass obtained from urban, domestic wastes and bio-wastes is a naturally plentiful resource with enormous potential as a source of raw materials for the generation of power, heat, and value-added chemicals with minimum gas emissions (Qian et al. 2015). Pyrolysis and gasification are commonly employed techniques to convert biomass to solid carbon residue called biochar (Shan et al. 2020; Zaimes et al. 2015). Recently, microwave-assisted pyrolysis (MWP) has emerged as a viable and eco-friendly technology for the efficient biochar production from biomass (Li et al. 2016). Biochar resulting from the thermal decomposition of biomass is a low-cost, carbon-dense substance that is considered in a sustainability context, since it enhances soil quality, effectively removes both organic and inorganic contaminants, and promotes carbon sequestration (Kookana et al. 2011; Tang et al. 2013; Xiong et al. 2017). Moreover, due to its economic synthesis (Jiang et al. 2023; Oni et al. 2019; Owsianiak et al. 2021), maneuverability characteristics, and sustainability benefits, biochar applications have recently been expanding to high-end industries including the energy and healthcare sectors (Ok et al. 2015). Considering these important uses, biochar chemistry has recently attracted impressive public and scientific attention, so the discovery of new applications is still very much in demand in both academia and industrial research. Despite all these applications and unique properties such as the abundance of surface functional groups, easily tunable surface functionality and porosity, the handling of biochar or modified biochar in the field of catalysts has been studied in a limited area: biodiesel production (Azman et al. 2023; Bazargan et al. 2015; Chong et al. 2021; da Luz Corrêa et al. 2023; Jayaraju et al. 2022; Li et al. 2014; Maroa and Inambao 2021; Tobío-Pérez et al. 2022; Velusamy et al. 2021) removal and/or mitigation of tar (Kastner et al. 2015; Shen and Fu 2018; Tian et al. 2021; Tian et al. 2022a, b), syngas production (Wang et al. 2022; Xu et al. 2022; Yang et al. 2022), and bio-oil upgrading (Liu et al. 2021; Qiu et al. 2020; Wu et al. 2021). Besides, there have been a few reports concerning the use of biochar as a platform for organic transformations or catalyst support (Chhabra et al. 2022; Dong et al. 2022a, b; Jenie et al. 2020a, b; Lyu et al. 2020; Moradi and Hajjami 2022; Sadjadi et al. 2019a, b; Steingruber et al. 2020; Tian et al. 2022a; Vidal et al. 2019; Vidal et al. 2021; Wang et al. 2023a; Zhang et al. 2022b) Compared to other carbocatalysts widely utilized in organic synthesis, such as carbon nanotubes (Corcho-Valdés et al. 2022; John et al. 2012),

carbon nanofibers (Kulkarni et al. 2022; Ruiz-Cornejo et al. 2020), graphene (Pandey et al. 2023; Zhang et al. 2022a), graphene oxide (GO) (Brisebois and Siaj 2020; Gao et al. 2022), and carbon nitrides (Suja et al. 2023; Wang et al. 2023b), the catalytic potential of biochar is relatively nascent. While these aforementioned carbon-based catalysts have demonstrated promising catalytic applications, biochar's catalytic uses are still in the early stages of development and to achieve commercialization, further research and development are needed for practical applications in diverse catalytic processes. So, extending the current approaches towards enhancing the progress of application-oriented biochar catalysts within the field of organic transformations is highly advantageous.

In the last decade, the concept of multicomponent reactions (MCRs) has garnered considerable enthusiasm within the scientific community owing to their exceptional synthetic efficiency and great atom economy (Cioc et al. 2014; Veisi et al. 2023). MCR approach offers a highly flexible synthetic toolbox that enables access to a library of substituted heterocyclic systems and complex molecules in a convergent way (Chen et al. 2019; Ibarra et al. 2018). It is obvious that the implementation of such strategies using green chemistry related materials such as natural acid/base catalysts (Ballini et al. 2000; Gupta and Paul 2014; Mohamadpour 2020; Patil et al. 2012), biopolymers (Shaabani and Maleki 2007), carbonaceous catalysts (Rajesh et al. 2015; Singha et al. 2022), and biocatalysts (Jumbam and Masamba 2020) would allow the minimization of both waste generation and human labour costs (Jacobi von Wangelin et al. 2003).

Given the beneficial features associated with biochar as a safe carbocatalyst as well as our current interest in using carbon-based materials in organic synthesis (Khalili et al. 2020, 2021, 2019, 2022; Rousta et al. 2021), herein we disclose our efforts on biochar-mediated direct multicomponent synthesis of 4*H*-benzo[*h*]chromenes and pyranopyrazoles. Chromenes and pyranopyrazoles constitute an extremely important class of fused heterocycles due to their broad range of potential pharmaceutical and biological properties (Gourdeau et al. 2004; Kumar et al. 2012; Mamaghani and Hossein Nia 2021; Prabhakara et al. 2015). It is noteworthy that biochar has been utilized as a basic carbocatalyst for the multicomponent synthesis of structurally diverse heterocycles with satisfied yields, operational simplicity, and good tolerance. This appears to be the first report of such an application. The established catalytic system not only opens an avenue to access 4*H*-benzo[*h*]chromenes and pyranopyrazoles under mild conditions, but also exhibits numerous distinctive attributes associated with green organic synthesis such as recyclable catalyst and easy product separation.

2 Experiment

2.1 General: biochar production

Cow and sheep dung, licorice root pulp, and compost made from municipal garbage were all acquired from active animal husbandries in Darab, and Zarghan town, Fars province, respectively. Following collection, the raw materials underwent a 48-h air-drying period, were subsequently ground using a high-speed mechanical grinder, and then placed in an oven for 24 h at 105 °C. The powdered biomass underwent slow pyrolysis in an electric muffle furnace (Shimifan, F47) at the temperatures of 300 and 600 °C under limited oxygen conditions. The temperature was gradually increased from room temperature by 5 °C per minute until it reached the final temperature, which was maintained for 2 h to facilitate slow pyrolysis. The produced biochars were allowed to cool slowly and passed through a 0.5 mm sieve for uniformity (Boostani et al. 2019). The biochars obtained from the pyrolysis of cow manure at 300 °C and 600 °C, sheep manure at 300 °C and 600 °C, licorice pulp at 300 °C and 600 °C and municipal compost at 300 °C and 600 °C were denoted as CB300, CB600, SB300, SB600, LB300, LB600, MB300 and MB600, respectively.

General procedure for synthesis of 4H-benzo[h] chromenes: A mixture of aldehyde (1 mmol), malononitrile (1 mmol), α-naphthol (1 mmol) and CB600 (10 mg) in H_2O (2 mL) was stirred at room temperature. After being stirred at room temperature (optimal temperature, Table 3) for 10 h, the reaction mixture was filtered through a pad of Celite to remove the CB600. The removal of the solvent under vacuum, followed by recrystallization with ethanol/water, afforded the pure 4*H*-benzo[*h*]chromene derivatives.

General procedure for synthesis of pyrano[2,3-c]pyrazoles: Malononitrile (1.1 mmol), ethylacetoacetate (1 mmol), hydrazine hydrate (1 mmol) and CB600 (10 mg) were added to a solution of aldehyde (1 mmol) in EtOH (2 mL) at room temperature. After stirring at room temperature for 12 h, the resulting mixture was subjected to filtration via a pad of Celite to remove the CB600. The removal of the solvent under vacuum, followed by recrystallization with ethanol/water, afforded the pure pyranopyrazoles.

Potentiometric titration of biochar samples: In order to obtain the basicity constant, 1 mg of biochar sample was dispersed in 1.0 mL of distilled water as the stock solution. For potentiometric titration, 300 μL of stock solution of dispersed biochar dissolved in 8 ml distilled water that contained 0.1 M KCl to keep the ionic strength constant. The aqueous dispersion of biochar sample was

titrated with small increments of HCl 0.1 M, under stirring. The pH was monitored by a pH meter after each addition of titrant. The new portion of titrant was added when the pH was constant for ~ 20 s. Experimental values of pH vs volume, were fitted by Curve Expert program to obtain the pH at the midpoint of equivalent.

3 Results and discussion

The biochars were obtained from local sources (cow and sheep manure) and organic wastes (licorice pulp) through a slow pyrolysis process. Initially, the biomasses were air-dried, crushed using a mechanical grinder and then passed through a 2 mm sieve. Under low oxygen circumstances, slow pyrolysis was used to produce the biochars.(Additional file 1, Fig. S1) The prepared biochars were subjected to characterization through a series of analytical techniques, such as Fourier transform infrared (FT-IR) spectroscopy, energy-dispersive X-ray spectroscopy (EDX), scanning electron microscopy (SEM), and X-ray diffraction (XRD). The FTIR of the produced biochars (400–2000 cm^{-1}) was carried out and the pure CB300 powder exhibited characteristic absorption bands of -COOH groups (1612 cm^{-1}), lignin and cellulose functionalities (~1578, 1172 and 1016 cm^{-1}) (Boeriu et al. 2004; Keiluweit et al. 2010), Si–O (1159 cm^{-1}), calcium carbonate (1788, 1440, 872 and 712 cm^{-1}) (Bruckman and Wriessnig 2013), and phosphate functional groups in calcium hydroxyapatite (1098, and 618 cm^{-1}) (Trinkunaite-Felsen et al. 2014) (Fig. 1). Whereas, the CB600 exhibited much lower absorption bands of higher intensity that pertained to –COOH groups, lignin and cellulose functionalities, as well as phosphates. In accordance with the previous findings (Cao and Harris 2010), for the sample annealed at 600 °C (CB600; increasing charring temperature), the $CaCO_3$ peaks steadily increase in intensity, mainly due to the increasing amounts of crystalline calcium carbonate in the sample (Boostani et al. 2021). A quite similar pattern of absorption bands was observed for the other biochars.

The SEM images of different biochars are depicted in Fig. 2. For CB300, the image taken at ~1000 magnification showed disordered pores in the structure of biochar while at ~3000 magnification of CB600, the SEM image showed clearly more ordered pores in its structure. The images obtained for LB600 and MB600 exhibited a conspicuous presence of well-defined tubular pores that were closely adhered to the walls of specific particles. As can be seen from these SEM images, the macro-cellular organization of the original plant tissues is still discernible. It was also revealed that increasing pyrolysis temperature led to the increase in porosity biochar structure. This is due to the biochar being formed at higher temperatures having less volatile organic content and more minerals

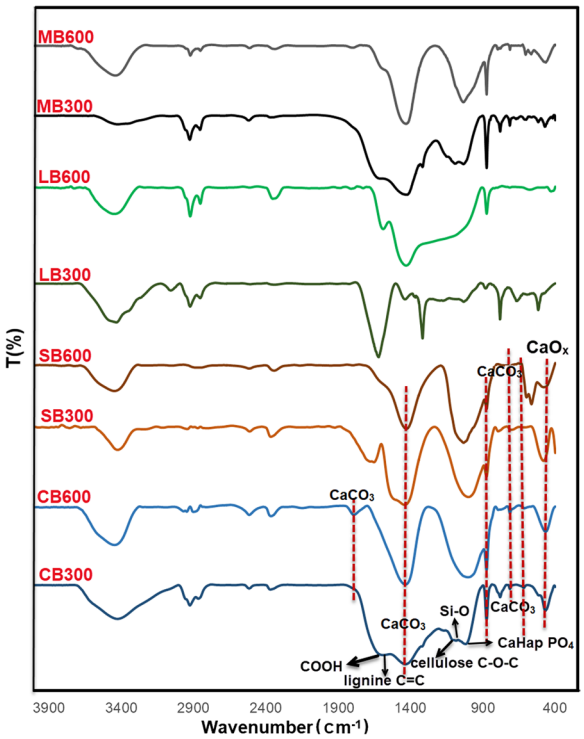

Fig. 1 FTIR spectra of CB600, CB300, SM300, SM600, LB300, LB600, MB300 and MB600

and black C structures crystallize (Cao and Harris 2010; Ma et al. 2016). Furthermore, it has been reported that increasing the pyrolysis temperature results in the dehydroxylation and the removal of aliphatic groups within the biochar structure, subsequently facilitating pore formation through the concurrent formation of fused-ring structures (Bagreev et al. 2001; Kloss et al. 2012) The structural morphology of biochars at 300 °C was relatively compact. The SEM–EDX of all biochars revealed rich amount of mineral elements (Additional file 1, Fig. S2).

The chemical structure and the crystallinity of the synthesized biochars were further characterized by X-ray powder diffraction (XRD) as shown in Fig. 3. The XRD patterns of the CB300 and CB600 display peaks corresponding to the quartz (SiO_2) crystalline compounds at around 2θ = 21.2, 26.5 and 51.7 (Bayarjargal et al. 2021; Han et al. 2017). The identification of quartz serves as clear evidence that the original feedstocks were abundant in Si, which is further supported by the Si–O–Si stretching band observed in the FT-IR spectra. The X-ray diffraction spectra of SB, LB, and MB biochars exhibited identical peaks.

The identification of calcite ($CaCO_3$) in biochars produced at two different temperatures was determined through the observation of peaks at 2θ = ~28, ~39.5,

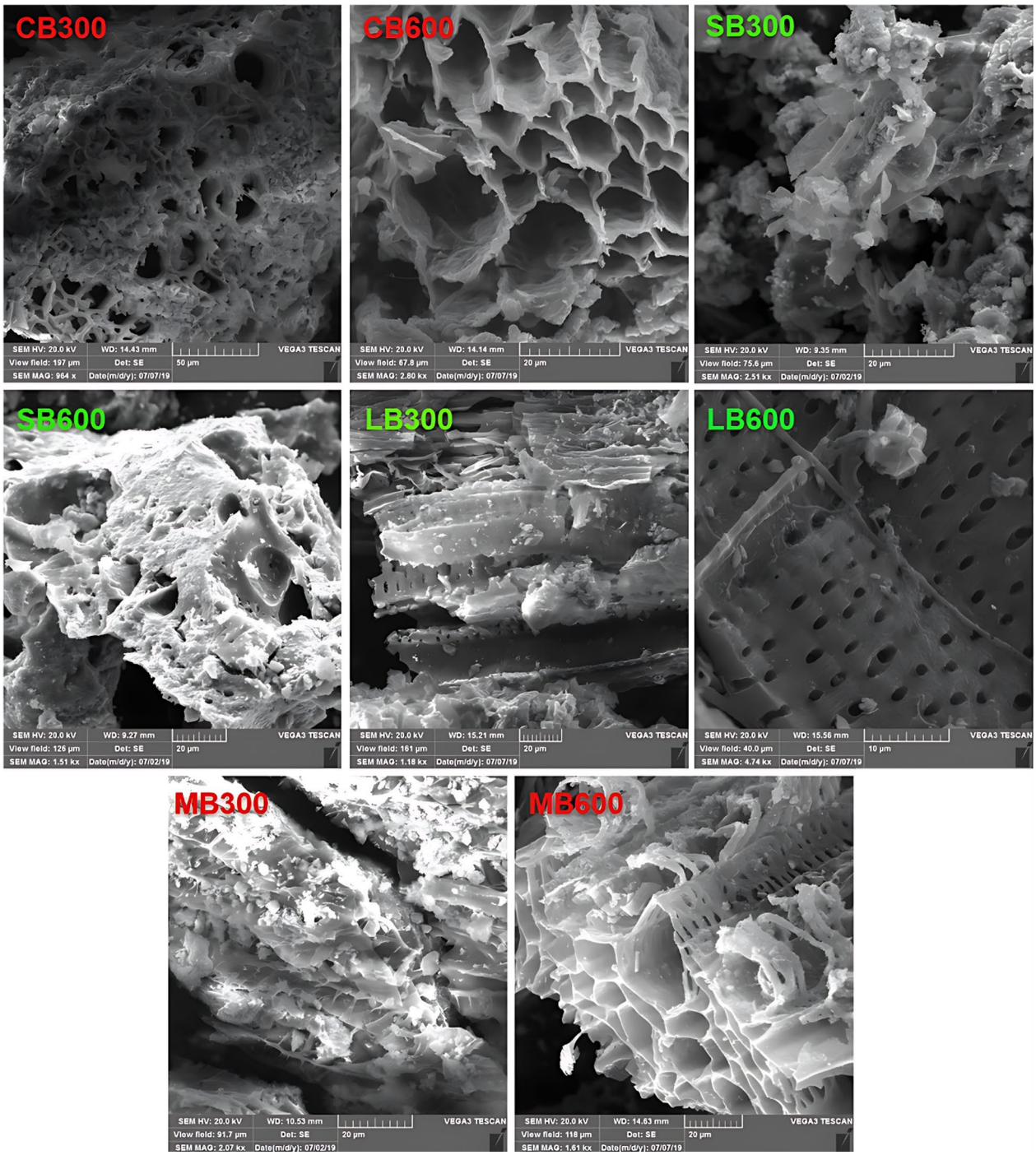

Fig. 2 SEM images of cow manure biochars produced at 300 °C (CB300), 600 °C (CB600), sheep manure biochar at 300 °C (SB300), 600 °C (SB600), licorice root pulp biochars at 300 °C (LB300), 600 °C (LB600), and municipal compost biochars at 300 °C (MB300) and 600 °C (MB600)

and ~ 47, as reported in previous studies (Kong and Liu 2019; Xie et al. 2022; Zhang et al. 2021). The presence of $Ca_3(PO_4)_2$ was confirmed through the observation of two peaks at $2\theta = 37°$ and 68°, which were consistent with literature. (Yu et al. 2021) Unknown and smaller weak peaks indicated the miscellaneous inorganic compounds. The chemical characteristics of the prepared biochars were also investigated using established laboratory methods. The pH values were measured in a suspension containing a 1:10 ratio of solid to distilled water, while the

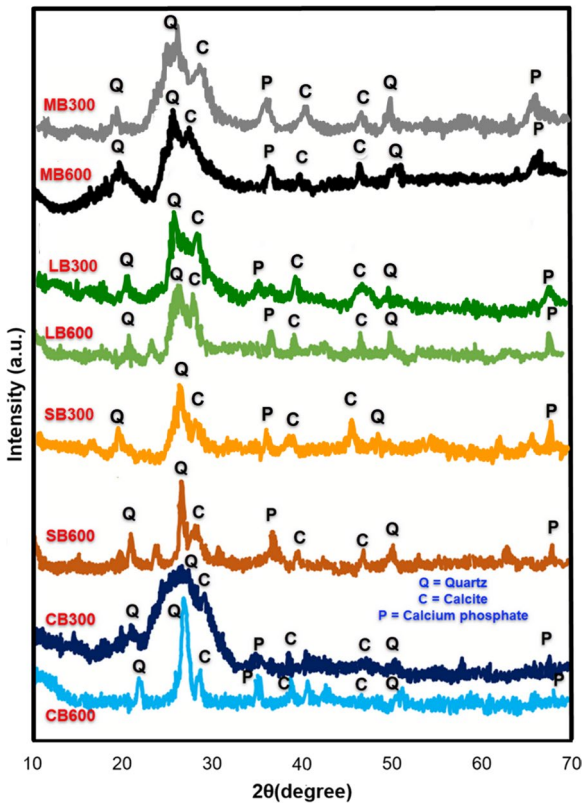

Fig. 3 Comparison of the XRD patterns of cow manure biochars produced at 300 °C (CB300), 600 °C (CB600), sheep manure biochar at 300 °C (SB300), 600 °C (SB600), licorice root pulp biochars at 300 °C (LB300), 600 °C (LB600), and municipal compost biochars at 300 °C (MB300) and 600 °C (MB600). Q, C, and P represents features of quartz, calcite and calcium phosphate

Table 1 Chemical properties of the biochars

Properties	CB300	CB600	SB600	LB600	MB600
H:C molar ratio	0.50	0.10	0.25	0.20	0.05
pH	10.73	11.51	10.32	9.38	10.64
Carbon (%)	53.14	57.30	52.74	72.92	52.76
Hydrogen (%)	2.63	0.82	1.19	1.34	0.34
Nitrogen (%)	3.05	2.12	2.84	2.65	2.81
Ash content (%)	25.32	48.86	54.26	23.43	41.97
S_{BET} (m^2 g^{-1})	67.6	85.4	35.2	51.5	78.8

CB300 denotes cow manure biochar produced at 300 °C; CB600 denotes cow manure biochar produced at 600 °C; SB600 denotes sheep manure biochar produced at 600 °C; LB600 denotes licorice root pulp biochar produced at 600 °C; MB600 denotes municipal compost biochar at 600 °C

CHN Analyzer was utilized to determine the percentage of total carbon (C), hydrogen (H), and nitrogen (N).

As shown in Table 1, all of the prepared biochars had a H:C mole ratio of 0.7 or less and 50% or greater total carbon content, making them all sufficiently pyrolyzed to qualify as biochars (According to the EBC and International Biochar Initiative (IBI)) (Comparison of European Biochar Certificate Version 4. 8 and IBI Biochar Standards Version 2. 0 European Biochar Certificate first publication March 2012 2012) The H:C mole ratio of the biochars also provides information about their aromaticity and degree of carbonization (Krull et al. 2021). A lower value of H:C mole ratio indicates a greater degree of aromatic condensation and carbonization. Among the studied biochars, CB600 and MB600 had the lowest H:C ratio and were the most carbonized biochars. By comparing the CB300 and CB600, it is evident that an increase in pyrolysis temperature from 300°C to 600°C results in a proportional increase in the degree of carbonization, as well as the C/H ratio. Comparing the pH values of CB300 and CB600 shows that with the increase of charring temperature, pH value elevates from 10.73 to 11.51. The pH rise can be attributed to the pyrolysis-induced increase in the amount of crystalline calcium carbonate, ash content, and the loss of surface acidic functional groups (Reeves et al. 2007). Such findings are supported by increasing the intensity of $CaCO_3$ peaks in IR spectrum of CB600. The findings indicate that the biochars had an alkaline pH, with values ranging from 9.38 to 11.51; the CB600 had the highest pH value (11.51), while the LB600 had the lowest (9.38). Generally, animal manures typically have substantially lower C content because they have a much larger percentage of inorganic components (ash content) (Boostani et al. 2018; Ro et al. 2010). The ash content of cow manure (CB) and sheep manure (MB) biochars was found to be higher (48.86% and 54.26%) than that of licorice pulp (LB) biochar (23.4%), therefore it is expected that CB and SB show more basic character than LB (as a plant biomass). The texture features (surface area) of the produced biochars were also analyzed using the Brunauer–Emmett–Teller (BET) method (N_2 as a sorbate gas). Based on the nitrogen quantity adsorbed at different relative pressures, the surface areas of CB300, CB600, SB600, LB600 and MB600 were found to be 67.6, 85.4, 35.2, 51.5 and 78.8 m^2g^{-1}, respectively. On comparing S_{BET} of CB300 and CB600, it was clear that biochar surface area is greatly affected by the pyrolysis temperature: At a low temperatures (e.g., 300 °C), the surface area of cow manure biochar is less than 68 m^2g^{-1}. When the temperature is increased to 600 °C, this surface area increases sharply to more than 85 m^2g^{-1} (Brown et al. 2006; Liu et al. 2015). To support the obtained chemical properties and quantitatively assess the basicity of the prepared biochars, a series of potentiometric titration was performed (Dimiev et al. 2013). According to the protocol, the stock solution of samples (1 mg of CB300, CB600, SB600, LB600 and MB600 in 1 mL of distilled water) containing 0.1 M KCl was titrated with small increments of HCl 0.1 M, under stirring. The additional

Table 2 Basicity constant of bochars obtained by potentiometric method

Samples	CB300	CB600	SB600	LB600	MB600
pK_b	6.66	5.72	7.93	7.14	7.08

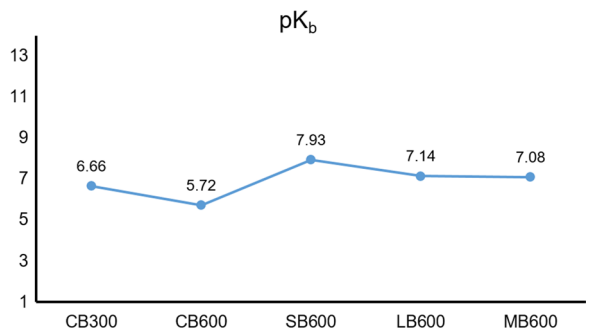

Fig. 4 pKb of the studied biochars

volume of titrant was added at the point of pH stabilization, which lasted approximately ~20 s. Experimental values of pH vs volume were fitted by Curve Expert program to obtain the pH at the midpoint of equivalent. Table 2 and Fig. 4 present the obtained basicity constants of the samples.

As evident from Table 2, typical data obtained for biochar titrations exhibit a substantial correlation with the chemical properties of the biochars. Among the studied materials, CB600 exhibited the most basicity as well as the largest pH.

After the characterization of the biochars, the catalytic activities of these carbon-based materials were examined in the multicomponent synthesis of 4*H*-benzo[*h*] chromenes. At the outset of this study, work on the optimization of the reaction conditions was focused on the catalyst and the solvent, using a model reaction of α-naphtol **1** (1.0 mmol), malonitrile **2** (1 mmol), and benzaldehyde (1 mmol), and the results are summarized in Table 3.

The control experiment showed that no product was detected over 24 h in the absence of the biochars under solvent-free conditions (Table 3, entry 1). The same result was observed when the model reaction was carried out without the biochars in H_2O as solvent (entry 2). Interestingly, a 56% yield of **4a** was achieved when the reaction was carried out by using 5 mg of CB300 (cow manure biochar produced at 300 °C) (entry 3). We then studied the influence of various biochars (Table 3, entries 4–7) and found that CB600 was superior to SB600, LB600, and MB600. An increase in CB600 loading to 10 mg resulted in a notable enhancement of the yield of product **4a**, as evidenced in entry 8 (87%). An important advantage of this simple catalytic system is that the model reaction also proceeded well at room temperature to afford excellent yield of the desired product (entry 9). To provide more insight into the efficiency of all the synthesized biochars, an investigation was conducted to assess the catalytic capabilities of the biochars (10 mg) in the multicomponent synthesis of 4*H*-benzo[*h*]chromenes **4a**, both at 70 °C and at room temperature. While all biochars gave poor-to- moderate product yields, only CB600 resulted in the quantitative formation of 4*H*-benzo[*h*]chromenes **4a** under the aforementioned reaction conditions (Table 1, entries 8–23). We have chosen to employ CB600 as the catalyst in the subsequent studies. Upon conducting the model reaction in the absence of solvent, it was observed that the resulting yield of **4a** was only 76%, as indicated in entry 24. Among the screened solvents, H_2O was found to be an effective solvent. As shown in Table 1, other organic solvents, such as toluene, THF, EtOH, CH_3CN and $CHCl_3$ had moderate activity, giving the desired product in 41–79% yields (entries 25–29). With respect to the catalyst loading, no significant improvement was observed with 15 mg of CB600 (entry 30). After determining the optimized reaction conditions, a diverse set of aldehydes was examined in conjunction with 1-naphtol and malonitrile to demonstrate the effectiveness and scope of this novel approach towards producing 4*H*-benzo[*h*]chromenes (Table 4). Generally, aldehydes bearing electron-rich and electron-deficient substituents underwent the multicomponent condensation smoothly to give the desired 4*H*-benzo[*h*]chromenes **4a–p** in good to excellent yields. It should be noted that aldehydes with electron-withdrawing groups, such as NO_2 and halogens on their *para*-positions gave the desired products with better yields than electron-poor substrates. On the other hand, aldehydes with halogen groups, such as Br, Cl, and F on their *para*-, and *meta*-positions also generated the corresponding products **4d–i** in 85–91% yields (entries 4–6, 8 and 9). It is obvious that an *ortho*-position effect with the sterically more hindered 2-chlorobenzaldehyde was observed in the reactions with **1** and **2** (entry 10). However, aldehydes bearing electron-rich substituents (–OMe, –OH, and –Me) on their *para*-, and *meta*-positions showed low reactivity (Table 4, entries 11–15) and the yields of the obtained desired products were 72–79%. Disubstituted aldehydes, such 3,4-dimethoxybenzaldehyde also underwent the condensation reaction and gave the corresponding product **4p** in 70% yield with an observed steric effect. However, the reaction of **1** and **2** with aliphatic aldehydes (such as butanal), and ketones (acetophenone) could not give the desired 4*H*-benzo[h] chromene product under the optimized reaction conditions.

Table 3 Optimization of reaction conditions

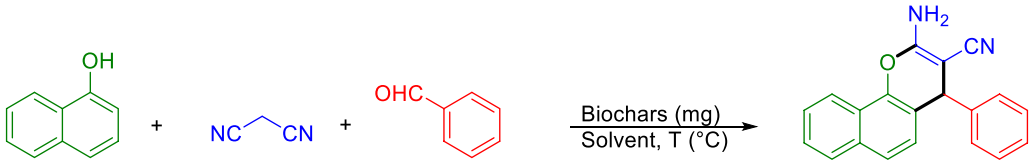

1 **2** **3a** **4a**

Entry	Catalyst (mg)	Solvent	T (°C)	Time (h)	Yield (%)[a]
1	–	–	70	24	–
2	–	H_2O	70	24	–
3	CB300 (5)	H_2O	70	18	56
4	CB600 (5)	H_2O	70	15	74
5	SB600 (5)	H_2O	70	15	67
6	LB600 (5)	H_2O	70	18	18
7	MB600 (5)	H_2O	70	15	60
8	CB600 (10)	H_2O	70	10	87
9[b]	**CB600 (10)**	**H_2O**	**r.t**	**10**	**84**
10	CB300 (10)	H_2O	70	12	68
11	CB300 (10)	H_2O	r.t	12	52
12	SB300 (10)	H_2O	70	12	62
13	SB 300 (10)	H_2O	r.t	12	55
14	SB600 (10)	H_2O	70	10	74
15	SB 600 (10)	H_2O	r.t	10	67
16	LB300 (10)	H_2O	70	18	14
17	LB300 (10)	H_2O	r.t	18	< 10
18	LB600 (10)	H_2O	70	18	31
19	LB600 (10)	H_2O	r.t	18	23
20	MB300 (10)	H_2O	70	15	60
21	MB300 (10)	H_2O	r.t	15	53
22	MB600 (10)	H_2O	70	12	70
23	MB600 (10)	H_2O	r.t	12	64
24	CB600 (10)	Solvent-free	r.t	12	76
25	CB600 (10)	Toluene	r.t	15	41
26	CB600 (10)	THF	r.t	15	59
27	CB600 (10)	EtOH	r.t	12	73
28	CB600 (10)	CH_3CN	r.t	12	79
29	CB600 (10)	$CHCl_3$	r.t	15	52
30	CB600 (15)	H_2O	r.t	10	85

Experimental conditions: α-naphtol **1** (1 mmol), malonitrile **2** (1 mmol), and benzaldehyde (1 mmol), Biochar (type indicated), and solvent (2.0 mL)

[a] Yield of pure isolated product

[b] Bold value signifies the best reaction conditions

To evaluate the present catalytic method on larger scales, we subsequently carried out the model reaction on a gram scale to demonstrate its utility. 4*H*-benzo[*h*] chromene (**4a**) was prepared using 5 mmol of materials under optimized conditions in 79% yield (Scheme 1).

In this study, a marginal decline in yield was recorded while synthesizing the desired product **4a**, however, more than 1 g of the final product **4a** could be obtained in less than 15 mL of water at room temperature. The most important aspect of a catalyst for its expanded use in industrial processes is its capacity to be recycled. The recovery of CB600 could be easily accomplished through simple filtration. Experimentally, after each run, the catalyst underwent recycling through filtration,

Table 4 CB600 mediated synthesis of 4*H*-benzo[h]chromenes[a]

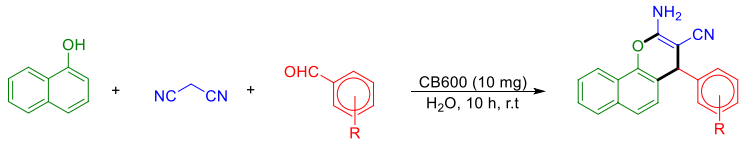

1 2 3a-p 4a-p

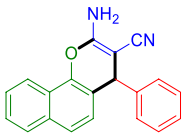

Entry 1: **4a**, 84%[b]

mp 215-217 ºC

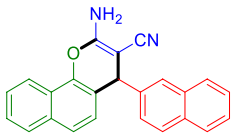

Entry 2: **4b**, 80%

mp 219-221 ºC

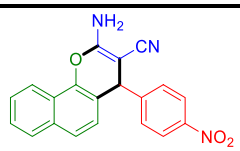

Entry 3: **4c**, 95%

mp 236-238 ºC

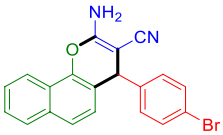

Entry 4: **4d**, 89%

mp 238-240 ºC

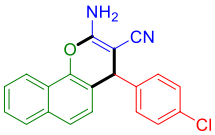

Entry 5: **4e**, 87%

mp 232-235 ºC

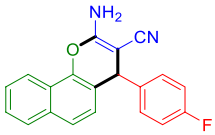

Entry 6: **4f**, 91%

mp 231-233 ºC

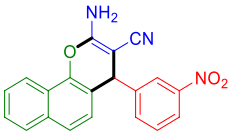

Entry 7: **4g**, 93%

mp 210-212 ºC

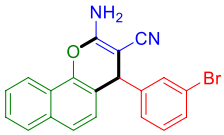

Entry 8: **4h**, 87%

mp 236-238 ºC

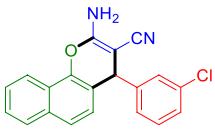

Entry 9: **4i**, 85%

mp 218-220 ºC

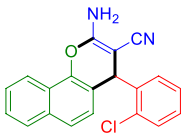

Entry 10: **4j**, 79%

mp 255-257 ºC

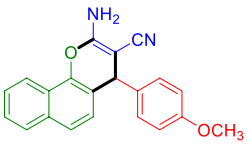

Entry 11: **4k**, 72%

mp 182-184 ºC

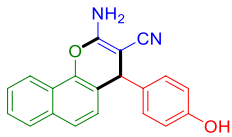

Entry 12: **4l**, 77%

mp 244-246 ºC

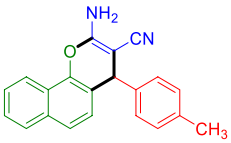

Entry 13: **4m**, 75%

mp 252-254 ºC

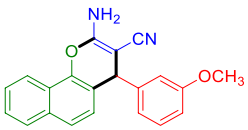

Entry 14: **4n**, 76%

mp 250-252 ºC

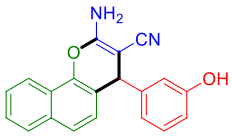

Entry 15: **4o**, 79%

mp 252-254 ºC

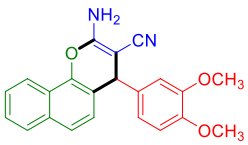

Entry 16: **4p**, 70%

mp 206-208 ºC

Table 4 (continued)

[a] Experimental conditions: α-naphtol **1** (1 mmol), malonitrile **2** (1 mmol), and aldehyde (1 mmol), CB600 (10 mg), and water (2.0 mL)

[b] Isolated yield

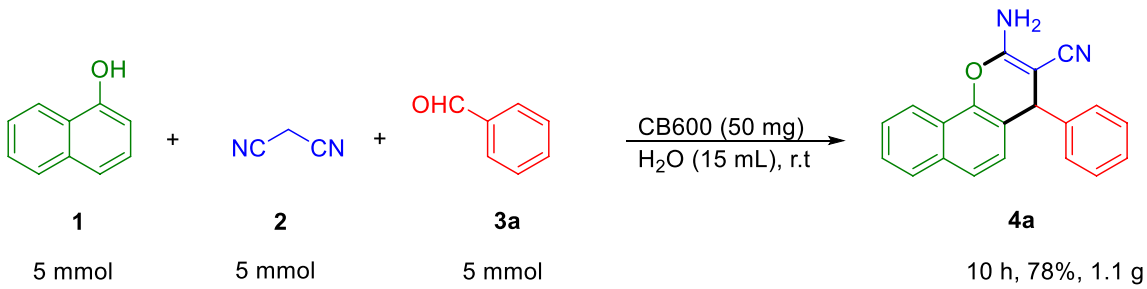

Scheme 1: Scheme Gram-Scale Synthesis of **4a**

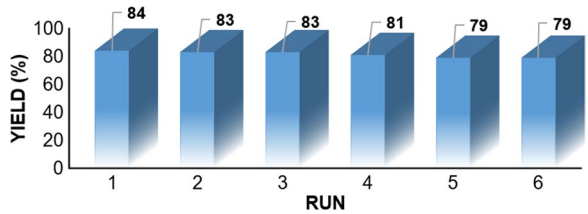

Fig. 5 Recycling of CB600. Conditions: α-naphtol **1** (3 mmol), malonitrile **2** (3 mmol), and benzaldehyde (3 mmol), CB600 (30 mg), and H_2O (5.0 mL)

followed by washing with ethanol (3 × 10 mL), air drying, and the subsequent application for the next run. The recycling test was conducted using the model reaction, indicating a slight loss of catalytic activity over six cycles (Fig. 5).

In order to conduct a more comprehensive assessment of the catalytic activity, the turnover numbers (TONs) and turnover frequency (TOF) of CB600 were calculated for the model reaction. The turnover numbers (TONs) were observed to be 5.9 under the given conditions. This catalytic system also afforded turnover frequencies (TOF) of 0.59 h^{-1}, which was high and acceptable (Ormsby et al. 2012; Xiong et al. 2017). Using the CB600-catalyzed reaction between α-naphtol **1**, malonitrile **2**, and benzaldehyde, as an example, the environmental factor (kg waste per kg product) (Sheldon 2007) of this catalytic system was 1.02 kg/kg (taking into account a loss of 10% of the solvent used). Atom economy is another significant green chemistry metric of the reaction that is frequently considered when assessing how "green" chemical processes are (Trost 1995). The atom economy (AE) of the present synthetic route was 94%. This value compares well with the AE of well-known MCR reactions (Cioc et al. 2014). These findings show that this novel effective catalytic system, optimized for the 4*H*-benzo[*h*]chromenes derivatives, could be of interest to pharmaceutical companies willing to create a more environmentally-friendly method of drug synthesis. We then monitored the fate of the catalyst in the model reaction after being reused. After the completion of the 6th cycle, the residual catalyst was isolated from the reaction mixture via filtration and the resulting carbon material was characterized by IR and XRD diffraction (Fig. 6a, b). As shown in Fig. 6, all peaks were preserved in the IR spectrum and XRD pattern of spent CB600, showing the active functional groups were kept in the recycled catalyst without substantial structural modifications. The results indicated that the catalyst exhibits stability and robustness when subjected to optimized reaction conditions. To evaluate the morphological alterations of the CB600 after being reused, the SEM and HRTEM images were obtained for the retrieved catalyst. SEM image of the reused catalyst showed less developed pore structures with more shrinkage or contraction after the 6th cycle. The TEM image of fresh CB600 in Fig. 6d (left) showed the presence of graphite-like structures at the edges of the biochar. As can be seen from TEM image, (Fig. 6d, right) the morphology of the spent catalyst showed a discernible degree of agglomeration, so the catalyst deactivation after six consecutive cycles has been attributed to the slight aggregation of the biochar layers. These findings demonstrated the stability and robustness of the introduced catalyst under optimized reaction conditions.

Encouraged by the successful outcomes achieved through the utilization of CB600 as a catalyst in the production of 4*H*-benzo[*h*]chromenes, and having high-yielding conditions in hands, we set out to optimize the reaction conditions for the synthesis of pyranopyrazoles. Considering the importance of pyranopyrazoles

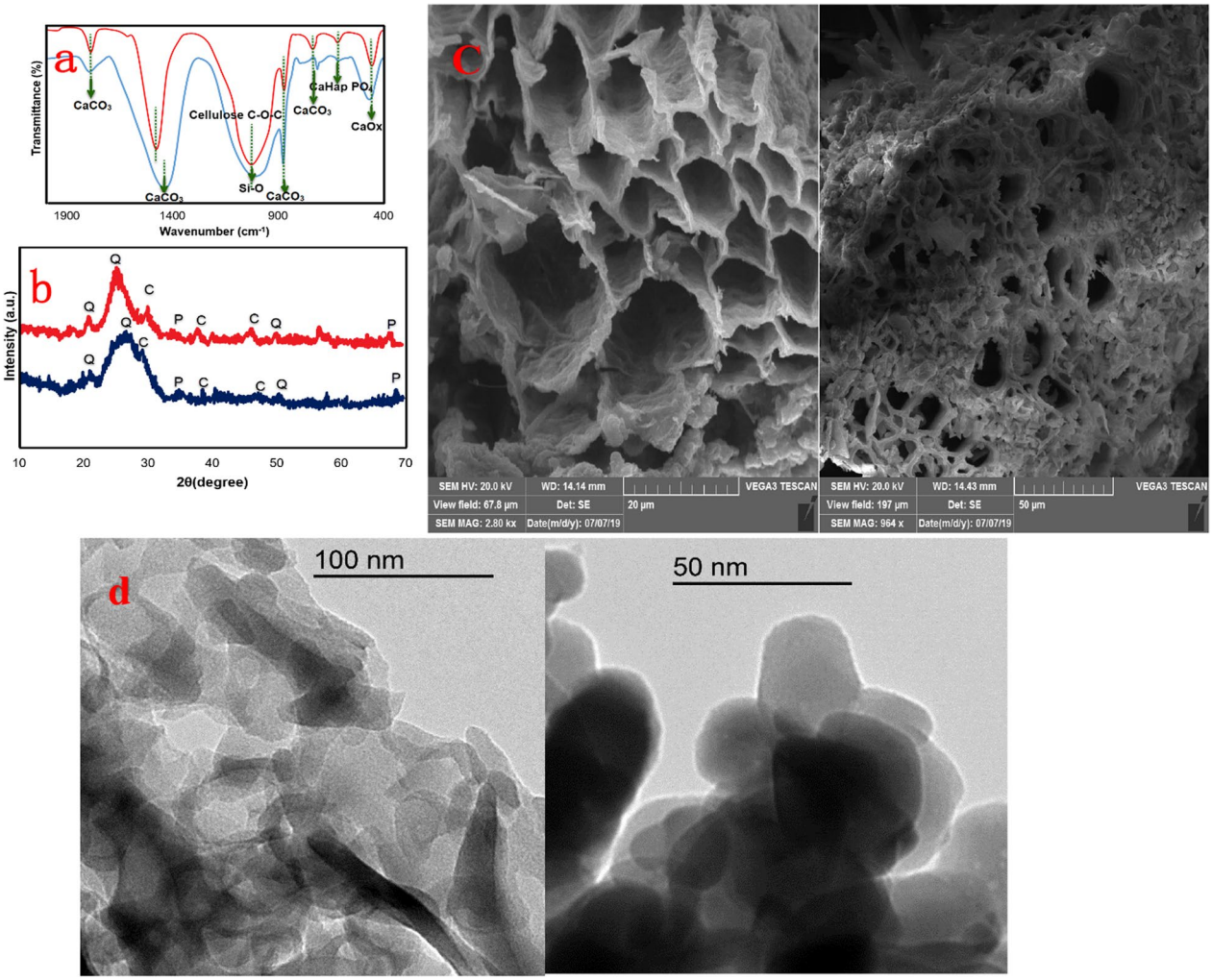

Fig. 6 **a** FT-IR spectra and (**b**) XRD patterns of fresh (blue) and six-times reused CB600 (red); (**c**) SEM and (**d**) HRTEM images of fresh (left) and reused (right) CB600

(Chougala et al. 2017; Reddy et al. 2019), numerous synthetic methods have been developed to produce these biologically significant heterocycles (Sikandar and Zahoor 2021). The one-pot reaction of β-ketoesters, hydrazine derivatives, substituted aldehydes, and malonitrile is a typical four-component approach to giving pyrano[2,3-c]pyrazole derivatives (Mamaghani and Hossein Nia 2021; Sikandar and Zahoor 2021). Therefore, the applicability of the biochars was examined for the synthesis of pyranopyrazoles using malonitrile **2** (1.1 mmol), benzaldehyde **3a** (1 mmol), ethyl acetoacetate **5** (1 mmol), and hydrazine hydrate **6** (1 mmol) as a model substrates. The outcome is summarized in Table 5.

It was found that the condensation of the reactants was not observed in the absence of either biochar or solvent, indicating that both of them are crucial for the reaction (Table 5, entries 1 and 2). To our delight, the desired product **7a** was formed in 24% isolated yield (Table 1, entry 1) with 10 mg of SB300. Further biochar screening suggested that CB600 is the best among different examined biochars (entries 3–10). These results align with the obtained basicity of the biochars in Table 2. Upon decreasing the temperature to ambient conditions, surprisingly, 85% of the desired product **7a** was obtained, indicating the nearly equal efficiency of these two examined temperatures (entry 11). The reaction could also proceed in other solvents, such as H_2O, CH_3CN, THF, and $CHCl_3$, albeit in lower yields (Table 1, entries 12–15). When catalyst loading was reduced to 5 mg, only 72% of the desired product was obtained (entry 16). Further, no improvement was observed when the model reaction was carried out with 15 mg of CB600 (entry 17). After sufficient screening, the optimal condition eventually emerged

Table 5 Optimization of reaction conditions for **7a**

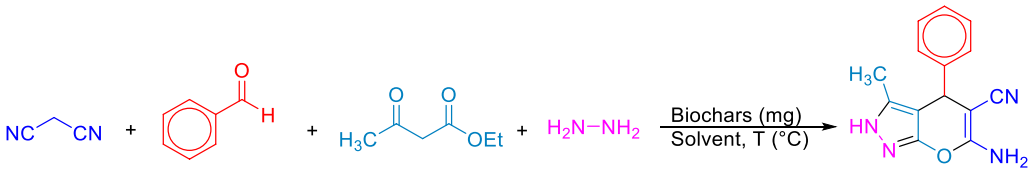

2 **3a** **5** **6** **7a**

Entry	Catalyst (mg)	Solvent	T (°C)	Time (h)	Yield (%)[a]
1	–	–	80	24	–
2	–	EtOH	Reflux	24	–
3	SB300 (10)	EtOH	Reflux	18	24
4	SB600 (10)	EtOH	Reflux	18	36
5	LB300 (10)	EtOH	Reflux	15	52
6	LB600 (10)	EtOH	Reflux	15	59
7	MB300 (10)	EtOH	Reflux	12	65
8	MB600 (10)	EtOH	Reflux	12	73
9	CB300 (10)	EtOH	Reflux	12	68
10	CB600 (10)	EtOH	Reflux	12	89
11[b]	**CB600 (10)**	**EtOH**	**r.t**	**12**	**85**
12	CB600 (10)	H_2O	r.t	12	68
13	CB600 (10)	CH_3CN	r.t	12	75
14	CB600 (10)	THF	r.t	12	57
15	CB600 (10)	$CHCl_3$	r.t	12	55
16	CB600 (5)	EtOH	r.t	12	72
17	CB600 (15)	EtOH	r.t	12	88

Experimental conditions: malonitrile **2** (1.1 mmol), and benzaldehyde (1 mmol), ethylacetoacetate **5** (1 mmol), hydrazine hydrate **6** (1 mmol) Biochar (type indicated), and solvent (2.0 mL).

[a] Yield of pure isolated product

[b] Bold value signifies the best reaction conditions

as malonitrile **2** (1.1 mmol), benzaldehyde **3a** (1 mmol), ethyl acetoacetate **5** (1 mmol), and hydrazine hydrate **6** (1 mmol) in the presence of a catalytic amount of CB600 (10 mg) at room temperature in ethanol (2 mL) for 12 h. By following the optimized conditions, a broad scope of aldehydes bearing different substituents (nitro, halogen, methoxy, hydroxyl, and methyl) was examined and gratifyingly all worked well and delivered expected pyranopyrazole products. Noting that aldehydes possessing an electron-deficient group on the aromatic ring exhibited a higher yield compared to those containing an electron-donating group on the aromatic ring. For example, the aromatic aldehydes with an electron-withdrawing groups on *para* and *meta*-position, such as NO_2 or halogens, reacted with malonitrile **2**, ethylacetoacetate **5** and hydrazine hydrate **6** to afford the corresponding products **7b–g** in almost quantitative yields (Table 6, entries 2–7). The yields of products **7h** and **7i** were low due to steric hindrance when Cl was positioned at the *ortho*-position of the phenyl rings, as indicated in entries 8 and 9. In contrast, the reactions with aldehydes bearing electron-donating groups furnished products **7j–o** in low to moderate yields (68–77%, Table 6, entries 10–15).

Interestingly, heterocyclic aldehydes such as pyridine-3-carbaldehyde could also be used in this MCR reaction to yield the final product **7p** in excellent yield (entry 16). Further experiments were performed to reinforce the benefit of this heterogeneous catalytic system using the model reaction. The results shown in Fig. 7 indicated that the recovered CB600 can be successfully reused in the subsequent five cycles with nearly unchanged catalytic activity, giving the desired product **7a** in good yields.

The CB600-catalyzed formation of pyrano[2,3-*c*]pyrazoles **7a** was characterized by turnover numbers (TONs), e.g., in the reaction between malonitrile, benzaldehyde, ethylacetoacetate, and hydrazine hydrate, it amounted to 12.5. Under these conditions, TOF was 5.0. The E-factor and atom economy of the catalytic system (Table 4, entry 1) were 1.3 kg kg^{-1}, and 75%, respectively. To check

Table 6 Substrate scope for pyrano[2,3-*c*]pyrazoles synthesis catalyzed by CB600

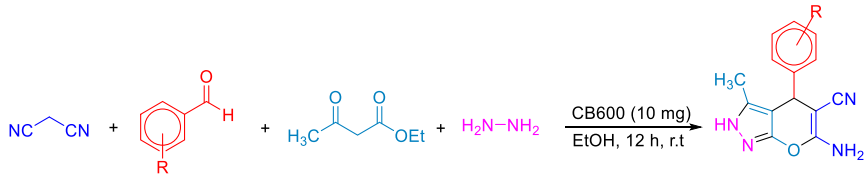

2 3 5 6 7a-p

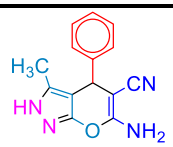

Entry 1: **7a**, 85%[b]

mp 244-246 ºC

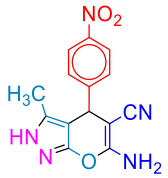

Entry 2: **7b**, 95%

mp 221-223 ºC

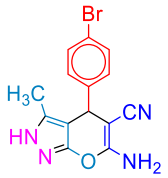

Entry 3: **7c**, 90%

mp 178-180 ºC

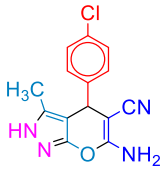

Entry 4: **7d**, 88%

mp 174-176 ºC

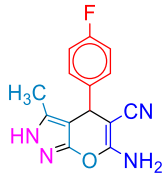

Entry 5: **7e**, 95%

mp 241-243 ºC

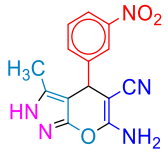

Entry 6: **7f**, 94%

mp 190-193 ºC

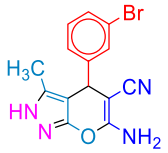

Entry 7: **7g**, 88%

mp 223-224 ºC

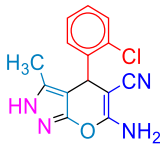

Entry 8: **7h**, 75%

mp 240-242 ºC

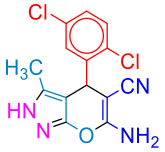

Entry 9: **7i**, 67%

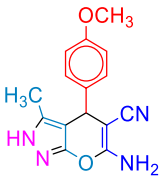

Entry 10: **7j**, 72%

mp 170-172 ºC

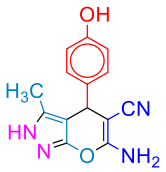

Entry 11: **7k**, 68%

mp 223-225 ºC

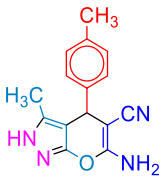

Entry 12: **7l**, 76%

mp 205-208 ºC

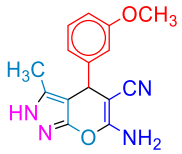

Entry 13: **7m**, 77%

mp 209-211 ºC

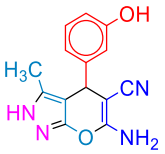

Entry 14: **7n**, 73%

mp 247-249 ºC

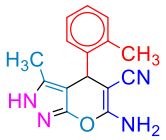

Entry 15: **7o**, 70%

208-210 ºC

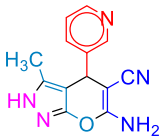

Entry 16: **7p**, 94%

mp 212-214

Experimental conditions: malonitrile **2** (1.1 mmol), aldehydes **3** (1 mmol), ethylacetoacetate **5** (1 mmol), and hydrazine hydrate **6** (1 mmol) CB600 (10 mg), and ethanol (2.0 mL) at room temperature. [b] isolated yield

the merit of the present work, we compared the catalytic performance of CB600 with some other reported basic catalytic systems in the literature used in the synthesis of 4*H*-benzo[*h*]chromenes **4a** (Table 7). These comparative results demonstrate the distinct advantage of utilizing heterogeneous BC600 over the currently employed methods (based on yield, reaction time, and reaction condition).

In terms of the experimental results and previous reports, the proposed mechanisms for the production of 4*H*-benzo[*h*]chromenes (Gangu et al. 2017; Khurana et al. 2010; Rahmatpour et al. 2022; Ren and Cai 2008)

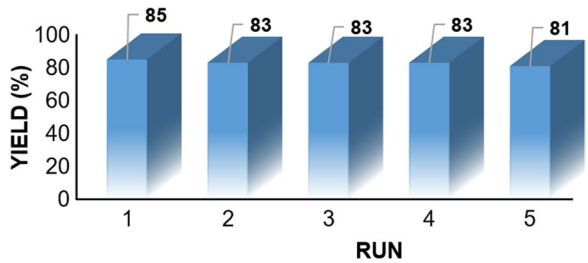

Fig. 7 Recycling of CB600. Experimental conditions: malonitrile **2** (3.3 mmol), benzaldehyde **3a** (3 mmol), ethylacetoacetate **5** (3 mmol), and hydrazine hydrate **6** (3 mmol) CB600 (30 mg), and Ethanol (5.0 mL) at room temperature

and pyranopyrazoles (Kargar et al. 2020; Saravana Ganesan and Suresh 2020; Shaabani et al. 2019) utilizing CB600 were depicted in Fig. 8. The mechanism of chromene synthesis can be conceptualized as a series of sequential reactions, involving Knoevenagel reaction, Michael addition and an intramolecular cyclization that may contribute to the generation of the final product. The reaction proceeds through the initial formation of α-cyanocinnamonitrile (**I**). Next, the Michael-type addition of α-naphthol to α-cyanocinnamonitrile results in the in-situ formation of the Michael addition product (**II**), which subsequently undergoes intramolecular nucleophilic cyclization to afford the desired 4*H*-benzo[*h*] chromenes.

Supporting evidence for the proposed mechanism was provided by independent reaction of α-cyano-4-chlorocinnamonitrile with α-naphthol in the presence of CB600, which gave the desired product 4*H*-benzo[*h*] chromenes **4e** in 91% yield (Khurana et al. 2010). α-Cyano-4-chlorocinnamonitrile was synthesized through Knoevenagel condensation of malononitrile and 4-chlorobenzaldehyde employing CB600 in water. In this reaction, a white precipitate was isolated which tentatively identified as 4-chlorobenzylidenemalonodinitrile. The ^{1}H and ^{13}C NMR spectra of this precipitate in DMSO-d6 confirmed its structure (SI). A plausible mechanism for pyranopyrazoles is outlined in Fig. 8b. Initially, the cyclocondensation of hydrazine with ethyl acetoacetate affords pyrazolone which is further rearranged into tautomer (**III**) via keto-enol tautomerization in the presence of CB600. Meanwhile, a Knoevenagel condensation of aldehyde with malononitrile promoted by CB600 gives α-cyanocinnamonitrile (**I**). Subsequently, the activation of pyrazolone by CB600 leads to the Michael addition to α-cyanocinnamonitrile (**I**) and subsequent cyclization and tautomerization (1,3-H shift) gives the desired pyranopyrazole. To investigate the role of CB600 in the reaction, a two-component reaction between ethyl acetoacetate and hydrazine was carried out in the presence and absence of CB600. It was observed that pyrazolone formation was instantaneous in the presence of CB600, whilst the same reaction occurred slowly without CB600. To establish the mechanism of the reaction, two involving intermediates, pyrazolone and the Knoevenagel adduct α-cyanocinnamonitrile (**I**) were prepared separately and characterized by the ^{1}H and ^{13}C NMR spectral analysis (SI). Control experiment involving the reaction of pyrazolone with α-cyanocinnamonitrile (**I**) under the optimized conditions afforded the desired pyranopyrazole **7a** in 89%

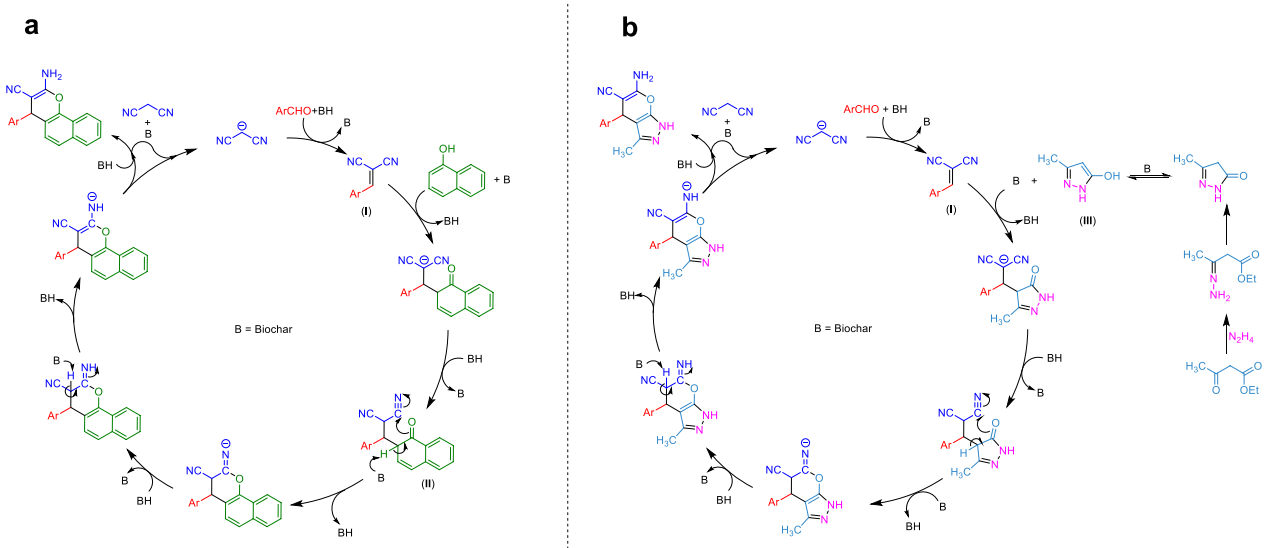

Fig. 8 Plausible mechanism for the synthesis of (**a**) 4*H*-benzo[*h*]chromenes and (**b**) pyranopyrazoles in the presence of CB600

Table 7 Comparative study of CB600 for the one-pot four-component synthesis of **4a**

Entry	Catalyst, conditions	Yield (%)	Refs.
1	CB600, H_2O, r.t., 10 h	84	This work
2	DBU, H_2O, reflux, 6 min	92	Khurana et al. (2010)
3	$Na_2CaP_2O_7$, H_2O, reflux, 5h	81	Solhy et al. (2010)
4	amino-functionalized MCM-41, H_2O, 70 °C, 0.5 h	80	Mirza-Aghayan et al. (2013)
5	Basic alumina, H_2O, 100 °C, 3 h	96	Maggi et al. (2004)
6	CeO2-CaO (25 mg), H_2O, 80 °C, 1 h	78	Samantaray et al. (2012)
7	Mg/Al hydrotalcite, MW, 140°C, 7 min	84	Surpur et al. (2009)
8	Imidazole, EtOH, reflux, 0.5 h	88	Khan et al. (2014)

yield. The obtained result confirms that the intermediates pyrazolone and α-cyanocinnamonitrile (**I**) are formed during the course of the present reaction. This observation is in accordance with those reported for the base-catalyzed pyrano[2,3-*c*]pyrazoles formation via one-pot four-component reactions (Azzam and Pasha 2012) (Table 7).

4 Conclusion

In summary, we have synthesized and characterized various nanobiochars through the pyrolysis-carbonization of different manures and organic wastes. The activity of these biochars was demonstrated through their use in two base-catalyzed reactions: multicomponent synthesis of 4*H*-benzo[*h*]chromene and pyranopyrazoles. Among the examined nanobiochars, cow manure biochar formed at 600 °C (CB600) was found to be the best solid-base heterogeneous catalyst for the tandem synthesis of 4*H*-benzo[*h*]chromenes and pyranopyrazoles under metal-free, mild and green condition. The outcomes of this research present new possibilities for the development of basic carbocatalysts from bio-wastes for multicomponent synthesis of structurally diverse heterocycles.

Supplementary Information

The online version contains supplementary material available at https://doi.org/10.1007/s42773-023-00286-y.

Additional file 1: Fig. S1 Generation of biochars via slow-pyrolysis of biomasses. **Fig. S2** EDX analysis of all produced biochars.

Acknowledgements
We gratefully acknowledge the financial support from Shiraz University.

Author contributions
DK: Conceptualization, methodology, formal analysis, investigation, supervision, writing-review and editing, project administration, funding acquisition. AAR: Methodology, formal analysis, investigation, data curation, Validation. HRB: Investigation, formal analysis, data curation, validation, review and editing. AG: Data analysis and review.

Dedication
This article is dedicated to Prof. Nasser Iranpoor and Prof. Habib Firouzabadi for their invaluable supports throughout our research journey.

Funding
The research leading to these results received funding from Shiraz University (Grant No. 0GRC1M235307).

Data availability
The datasets used or analyzed during the current study are available from the corresponding author on reasonable request.

Declarations

Competing Interests
The authors have no conflicts of interest to disclose, financial or otherwise.

Author details
[1]Department of Chemistry, College of Sciences, Shiraz University, Shiraz 71467-13565, Iran. [2]Department of Soil Science, College of Agriculture and Natural Resources of Darab, Shiraz University, Darab, Iran. [3]Department of Chemistry, College of Sciences, University of Hormozgan, Bandar Abbas 7916193145, Iran.

Received: 4 May 2023 Revised: 12 November 2023 Accepted: 15 November 2023
Published online: 11 January 2024

References

Albers SC, Berklund AM, Graff GD (2016) The rise and fall of innovation in biofuels. Nat Biotechnol 34:814–821. https://doi.org/10.1038/nbt.3644
Azman NS, Khairuddin N, Tengku Azmi TSM, Seenivasagam S, Hassan MA (2023) Application of biochar from woodchip as catalyst support for biodiesel production. Catalysts 13:489. https://doi.org/10.3390/catal13030489
Azzam SHS, Pasha M (2012) Simple and efficient protocol for the synthesis of novel dihydro-1*H*-pyrano [2, 3-c] pyrazol-6-ones via a one-pot four-component reaction. Tetrahedron Lett 53:6834–6837. https://doi.org/10.1016/j.tetlet.2012.10.025
Bagreev A, Bandosz TJ, Locke DC (2001) Pore structure and surface chemistry of adsorbents obtained by pyrolysis of sewage sludge-derived fertilizer. Carbon 39:1971–1979. https://doi.org/10.1016/S0008-6223(01)00026-4
Ballini R, Bigi F, Conforti ML, De Santis D, Maggi R, Oppici G, Sartori G (2000) Multicomponent reactions under clay catalysis. Catal Today 60:305–309. https://doi.org/10.1016/S0920-5861(00)00347-3
Bayarjargal B, Nomuunzaya E-O, Sainzaya B, Saurjan T, Erdenedalai J, Buyan C (2021) Characterization of biochars produced from various biowastes. In: Proceedings of the 5th International Conference on Chemical

Investigation and Utilization of Natural Resource (ICCIUNR-2021), 2021/10/05 2021. Atlantis Press, pp 73–81. https://doi.org/10.2991/ahcps.k.211004.012
Bazargan A, Kostić MD, Stamenković OS, Veljković VB, McKay G (2015) A calcium oxide-based catalyst derived from palm kernel shell gasification residues for biodiesel production. Fuel 150:519–525. https://doi.org/10.1016/j.fuel.2015.02.046
Boeriu CG, Bravo D, Gosselink RJA, van Dam JEG (2004) Characterisation of structure-dependent functional properties of lignin with infrared spectroscopy. Ind Crops Prod 20:205–218. https://doi.org/10.1016/j.indcrop.2004.04.022
Boostani HR, Hardie AG, Najafi-Ghiri M, Khalili D (2018) Investigation of cadmium immobilization in a contaminated calcareous soil as influenced by biochars and natural zeolite application. J Environ Sci Technol 15:2433–2446. https://doi.org/10.1007/s13762-017-1544-3
Boostani HR, Najafi-Ghiri M, Hardie AG, Khalili D (2019) Comparison of Pb stabilization in a contaminated calcareous soil by application of vermicompost and sheep manure and their biochars produced at two temperatures. Appl Geochem 102:121–128. https://doi.org/10.1016/j.apgeochem.2019.01.013
Boostani HR, Hardie AG, Najafi-Ghiri M, Khalili D (2021) The effect of soil moisture regime and biochar application on lead (Pb) stabilization in a contaminated soil. Ecotoxicol Environ Saf 208:111626. https://doi.org/10.1016/j.ecoenv.2020.111626
Brisebois P, Siaj M (2020) Harvesting graphene oxide–years 1859 to 2019: a review of its structure, synthesis, properties and exfoliation. J Mater Chem C 8:1517–1547. https://doi.org/10.1039/C9TC03251G
Brown RA, Kercher AK, Nguyen TH, Nagle DC, Ball WP (2006) Production and characterization of synthetic wood chars for use as surrogates for natural sorbents. Org Geochem 37:321–333. https://doi.org/10.1016/j.orggeochem.2005.10.008
Bruckman VJ, Wriessnig K (2013) Improved soil carbonate determination by FT-IR and X-ray analysis. Environ Chem Lett 11:65–70. https://doi.org/10.1007/s10311-012-0380-4
Cao X, Harris W (2010) Properties of dairy-manure-derived biochar pertinent to its potential use in remediation. Bioresour Technol 101:5222–5228. https://doi.org/10.1016/j.biortech.2010.02.052
Chen M-N, Mo L-P, Cui Z-S, Zhang Z-H (2019) Magnetic nanocatalysts: synthesis and application in multicomponent reactions. Curr Opin Green Sustain Chem 15:27–37. https://doi.org/10.1016/j.cogsc.2018.08.009
Chhabra T, Dwivedi P, Krishnan V (2022) Acid functionalized hydrochar as heterogeneous catalysts for solventless synthesis of biofuel precursors. Green Chem 24:898–910. https://doi.org/10.1039/D1GC03330A
Chong CC, Cheng YW, Lam MK, Setiabudi HD, Vo D-VN (2021) State-of-the-art of the synthesis and applications of sulfonated carbon-based catalysts for biodiesel production: a review. Energy Technol 9:2100303. https://doi.org/10.1002/ente.202100303
Chougala BM et al (2017) Synthesis, characterization and molecular docking studies of substituted 4-coumarinylpyrano[2,3-c]pyrazole derivatives as potent antibacterial and anti-inflammatory agents. Eur J Med Chem 125:101–116. https://doi.org/10.1016/j.ejmech.2016.09.021
Cioc RC, Ruijter E, Orru RV (2014) Multicomponent reactions: advanced tools for sustainable organic synthesis. Green Chem 16:2958–2975. https://doi.org/10.1039/C4GC00013G
Comparison of European Biochar Certificate Version 4. 8 and IBI Biochar Standards Version 2.0 European Biochar Certificate first publication March 2012 (2012)
Corcho-Valdés AL, Iriarte-Mesa C, Calzadilla-Maya J, Matos-Peralta Y, Desdín-García LF, Antuch M (2022) Carbon nanotubes in organic catalysis carbon composite catalysts: preparation, structural and morphological property and applications. Springer, Singapore, pp 223–266. https://doi.org/10.1007/978-981-19-1750-9
da Luz Corrêa AP, da Silva PMM, Gonçalves MA, Bastos RRC, da Rocha Filho GN, da Conceição LRV (2023) Study of the activity and stability of sulfonated carbon catalyst from agroindustrial waste in biodiesel production: influence of pyrolysis temperature on functionalization. Arab J Chem 16:104964. https://doi.org/10.1016/j.arabjc.2023.104964
Dimiev AM, Alemany LB, Tour JM (2013) Graphene oxide. Origin of acidity, its instability in water, and a new dynamic structural model. ACS Nano 7:576–588. https://doi.org/10.1021/nn3047378
Dong L-N, Wang Y-M, Zhang W-L, Mo L-P, Zhang Z-H (2022a) Nickel supported on magnetic biochar as a highly efficient and recyclable heterogeneous catalyst for the one-pot synthesis of spirooxindole-dihydropyridines. Appl Organomet Chem 36:e6667. https://doi.org/10.1002/aoc.6667
Dong L-N, Zhang S-Z, Zhang W-L, Dong Y, Mo L-P, Zhang Z-H (2022b) Synthesis, characterization and application of magnetic biochar sulfonic acid as a highly efficient recyclable catalyst for preparation of spiro-pyrazolo [3, 4-b] pyridines. Res Chem Intermed 48:1249–1272. https://doi.org/10.1007/s11164-022-04660-6
Gangu KK, Maddila S, Mukkamala SB, Jonnalagadda SB (2017) Synthesis, structure, and properties of new Mg (II)-metal–organic framework and its prowess as catalyst in the production of 4 H-Pyrans. Ind Eng Chem Res 56:2917–2924. https://doi.org/10.1021/acs.iecr.6b04795
Gao F, Zhang S, Lv Q, Yu B (2022) Recent advances in graphene oxide catalyzed organic transformations. Chin Chem Lett 33:2354–2362. https://doi.org/10.1016/j.cclet.2021.10.081
Gourdeau H et al (2004) Antivascular and antitumor evaluation of 2-amino-4-(3-bromo-4,5-dimethoxy-phenyl)-3-cyano-4*H*-chromenes, a novel series of anticancer agents. Mol Cancer Ther 3:1375–1384. https://doi.org/10.1158/1535-7163.1375.3.11
Gupta P, Paul S (2014) Solid acids: green alternatives for acid catalysis. Catal Today 236:153–170. https://doi.org/10.1016/j.cattod.2014.04.010
Han L, Qian L, Liu R, Chen M, Yan J, Hu Q (2017) Lead adsorption by biochar under the elevated competition of cadmium and aluminum. Sci Rep 7:2264. https://doi.org/10.1038/s41598-017-02353-4
Ibarra IA, Islas-Jácome A, González-Zamora E (2018) Synthesis of polyheterocycles via multicomponent reactions. Org Biomol Chem 16:1402–1418. https://doi.org/10.1039/C7OB02305G
Jacobi von Wangelin A, Neumann H, Gördes D, Klaus S, Strübing D, Beller M (2003) Multicomponent coupling reactions for organic synthesis: chemoselective reactions with amide–aldehyde mixtures. Chem A Eur J 9:4286–4294. https://doi.org/10.1002/chem.200305048
Jayaraju RM et al (2022) Biochar from waste biomass as a biocatalyst for biodiesel production: an overview. Appl Nanosci 12:3665–3676. https://doi.org/10.1007/s13204-021-01924-2
Jenie SA, Kristiani A, Khaerudini DS, Takeishi K (2020a) Sulfonated magnetic nanobiochar as heterogeneous acid catalyst for esterification reaction. J Environ Chem Eng 8:103912. https://doi.org/10.1016/j.jece.2020.103912
Jenie SNA, Kristiani A, Sudiyarmanto KDS, Takeishi K (2020b) Sulfonated magnetic nanobiochar as heterogeneous acid catalyst for esterification reaction. J Environ Chem Eng 8:103912. https://doi.org/10.1016/j.jece.2020.103912
Jiang M et al (2023) Nanobiochar for the remediation of contaminated soil and water: challenges and opportunities. Biochar 5:2. https://doi.org/10.1007/s42773-022-00201-x
John J, Gravel E, Namboothiri IN, Doris E (2012) Advances in carbon nanotube-noble metal catalyzed organic transformations. Nanotechnol Rev 1:515–539. https://doi.org/10.1515/ntrev-2012-0025
Jumbam ND, Masamba W (2020) Bio-catalysis in multicomponent reactions. Molecules 25:5935. https://doi.org/10.3390/molecules25245935
Kargar PG, Bagherzade G, Eshghi H (2020) Novel biocompatible core/shell Fe_3O_4@ NFC@ Co (ii) as a new catalyst in a multicomponent reaction: an efficient and sustainable methodology and novel reusable material for one-pot synthesis of 4 H-pyran and pyranopyrazole in aqueous media. RSC Adv 10:37086–37097. https://doi.org/10.1039/D0RA04698A
Kastner JR, Mani S, Juneja A (2015) Catalytic decomposition of tar using iron supported biochar. Fuel Process Technol 130:31–37. https://doi.org/10.1016/j.fuproc.2014.09.038
Keiluweit M, Nico PS, Johnson MG, Kleber M (2010) Dynamic molecular structure of plant biomass-derived black carbon (Biochar). Environ Sci Technol 44:1247–1253. https://doi.org/10.1021/es9031419
Khalili D, Rezaei M, Koohgard M (2019) Ligand-free copper-catalyzed O-arylation of aryl halides using impregnated copper ferrite on mesoporous graphitic carbon nitride as a robust and magnetic heterogeneous catalyst. Microporous Mesoporous Mater 287:254–263. https://doi.org/10.1016/j.micromeso.2019.06.007
Khalili D, Lavian S, Moayyed M (2020) Graphene oxide as a catalyst for one-pot sequential aldol coupling/aza-Michael addition of amines to chalcones through in situ generation of Michael acceptors under neat conditions.

Tetrahedron Lett 61:151470. https://doi.org/10.1016/j.tetlet.2019.151470
Khalili D, Rezaee M, Koohgard M (2021) Impregnated copper ferrite on mesoporous graphitic carbon nitride: a high-performance heterogeneous catalyst for A3-coupling reaction. ChemistrySelect 6:10619–10624. https://doi.org/10.1002/slct.202102586
Khalili D, Rousta M, Khalafi-Nezhad A, Ebrahimi E (2022) From methylarenes to esters: efficient oxidative Csp3–H activation promoted by CuO decorated magnetic reduced graphene oxide. New J Chem 46:14052–14064. https://doi.org/10.1039/D2NJ00728B
Khan MN, Pal S, Karamthulla S, Choudhury LH (2014) Imidazole as organocatalyst for multicomponent reactions: diversity oriented synthesis of functionalized hetero-and carbocycles using in situ-generated benzylidenemalononitrile derivatives. RSC Adv 4:3732–3741. https://doi.org/10.1039/C3RA45252B
Khurana JM, Nand B, Saluja P (2010) DBU: a highly efficient catalyst for one-pot synthesis of substituted 3, 4-dihydropyrano [3, 2-c] chromenes, dihydropyrano [4, 3-b] pyranes, 2-amino-4H-benzo [h] chromenes and 2-amino-4H benzo [g] chromenes in aqueous medium. Tetrahedron 66:5637–5641. https://doi.org/10.1016/j.tet.2010.05.082
Kloss S et al (2012) Characterization of slow pyrolysis biochars: effects of feedstocks and pyrolysis temperature on biochar properties. J Environ Qual 41:990–1000. https://doi.org/10.2134/jeq2011.0070
Kong W, Liu J (2019) Nitrogen-decorated, porous carbons derived from waste cow manure as efficient catalysts for the selective capture and conversion of CO_2. RSC Adv 9:4925–4931. https://doi.org/10.1039/C8RA10497B
Kookana RS, Sarmah AK, Van Zwieten L, Krull E, Singh B (2011) Biochar application to soil. In: Sparks DL (ed) Agronomic and environmental benefits and unintended consequences, vol 112. Academic Press, USA, pp 103–143. https://doi.org/10.1016/B978-0-12-385538-1.00003-2
Krull ES, Baldock JA, Skjemstad JO, Smernik RJ (2021) Characteristics of biochar: organo-chemical properties. In: Lehmann J, Joseph S (eds) Biochar for environmental management, 2nd edn. Routledge, USA, p 976. https://doi.org/10.4324/9781849770552
Kulkarni D et al (2022) Surface functionalization of nanofibers: the multifaceted approach for advanced biomedical applications. Nanomaterials 12:3899. https://doi.org/10.3390/nano12213899
Kumar A, Lohan P, Aneja DK, Gupta GK, Kaushik D, Prakash O (2012) Design, synthesis, computational and biological evaluation of some new hydrazino derivatives of DHA and pyranopyrazoles. Eur J Med Chem 50:81–89. https://doi.org/10.1016/j.ejmech.2012.01.042
Li M, Zheng Y, Chen Y, Zhu X (2014) Biodiesel production from waste cooking oil using a heterogeneous catalyst from pyrolyzed rice husk. Bioresour Technol 154:345–348. https://doi.org/10.1016/j.biortech.2013.12.070
Li J et al (2016) Biochar from microwave pyrolysis of biomass: a review. Biomass Bioenergy 94:228–244. https://doi.org/10.1016/j.biombioe.2016.09.010
Liu W-J, Jiang H, Yu H-Q (2015) Development of biochar-based functional materials: toward a sustainable platform carbon material. Chem Rev 115:12251–12285. https://doi.org/10.1021/acs.chemrev.5b00195
Liu S et al (2021) Understanding the catalytic upgrading of bio-oil from pine pyrolysis over CO_2-activated biochar. Renew Energy 174:538–546. https://doi.org/10.1016/j.renene.2021.04.085
Lyu H, Zhang Q, Shen B (2020) Application of biochar and its composites in catalysis. Chemosphere 240:124842. https://doi.org/10.1016/j.chemosphere.2019.124842
Ma X et al (2016) Study of biochar properties by scanning electron microscope–-energy dispersive X-ray spectroscopy (SEM-EDX). Commun Soil Sci Plant Anal 47:593–601. https://doi.org/10.1080/00103624.2016.1146742
Maggi R, Ballini R, Sartori G, Sartorio R (2004) Basic alumina catalysed synthesis of substituted 2-amino-2-chromenes via three-component reaction. Tetrahedron Lett 45:2297–2299. https://doi.org/10.1016/j.tetlet.2004.01.115
Mamaghani M, Hossein Nia R (2021) A review on the recent multicomponent synthesis of pyranopyrazoles polycyclic. Aromat Compd 41:223–291. https://doi.org/10.1080/10406638.2019.1584576
Maroa S, Inambao F (2021) A review of sustainable biodiesel production using biomass derived heterogeneous catalysts. Eng Life Sci 21:790–824. https://doi.org/10.1002/elsc.202100025
Mirza-Aghayan M, Nazmdeh S, Boukherroub R, Rahimifard M, Tarlani A, Abolghasemi-Malakshah M (2013) Convenient and efficient one-pot method for the synthesis of 2-amino-tetrahydro-4 H-chromenes and 2-amino-4 H-benzo [h]-chromenes using catalytic amount of amino-functionalized MCM-41 in aqueous media. Synth Commun 43:1499–1507. https://doi.org/10.1080/00397911.2011.643438
Mohamadpour F (2020) Green and convenient one-pot access to polyfunctionalized piperidine scaffolds via glutamic acid catalyzed Knoevenagel-intramolecular [4+ 2] aza-Diels-Alder imin-based multi-component reaction under ambient temperature. Polycyclic Aromat Compd 40:681–692. https://doi.org/10.1080/10406638.2018.1472111
Moradi P, Hajjami M (2022) Stabilization of ruthenium on biochar-nickel magnetic nanoparticles as a heterogeneous, practical, selective, and reusable nanocatalyst for the Suzuki C–C coupling reaction in water. RSC Adv 12:13523–13534. https://doi.org/10.1039/D1RA09350A
Ok YS, Chang SX, Gao B, Chung H-J (2015) SMART biochar technology—a shifting paradigm towards advanced materials and healthcare research. Environ Technol Innovation 4:206–209. https://doi.org/10.1016/j.eti.2015.08.003
Oni BA, Oziegbe O, Olawole OO (2019) Significance of biochar application to the environment and economy. Ann Agric Sci 64:222–236. https://doi.org/10.1016/j.aoas.2019.12.006
Ormsby R, Kastner JR, Miller J (2012) Hemicellulose hydrolysis using solid acid catalysts generated from biochar. Catal Today 190:89–97. https://doi.org/10.1016/j.cattod.2012.02.050
Owsianiak M, Lindhjem H, Cornelissen G, Hale SE, Sørmo E, Sparrevik M (2021) Environmental and economic impacts of biochar production and agricultural use in six developing and middle-income countries. Sci Total Environ 755:142455. https://doi.org/10.1016/j.scitotenv.2020.142455
Pandey G et al (2023) Graphene-based composite materials as catalyst for organic transformations. ChemistrySelect 8:e202203186. https://doi.org/10.1002/slct.202203186
Patil S, Jadhav S, Patil U (2012) Natural acid catalyzed synthesis of Schiff base under solvent-free condition: as a green approach. Arch Appl Sci Res 4:1074–1078
Prabhakara CT, Patil SA, Kulkarni AD, Naik VH, Manjunatha M, Kinnal SM, Badami PS (2015) Synthesis, spectral, thermal, fluorescence, antimicrobial, anthelmintic and DNA cleavage studies of mononuclear metal chelates of bi-dentate 2H-chromene-2-one Schiff base. J Photochem Photobiol, B 148:322–332. https://doi.org/10.1016/j.jphotobiol.2015.03.033
Qian K, Kumar A, Zhang H, Bellmer D, Huhnke R (2015) Recent advances in utilization of biochar. Renew Sust Energ Rev 42:1055–1064. https://doi.org/10.1016/j.rser.2014.10.074
Qiu Z et al (2020) Catalytic co-pyrolysis of sewage sludge and rice husk over biochar catalyst: bio-oil upgrading and catalytic mechanism. J Waste Manag 114:225–233. https://doi.org/10.1016/j.wasman.2020.07.013
Rahmatpour F, Kosari M, Monadi N (2022) Catalytic performance of copper (II) Schiff base complex immobilized on Fe_3O_4 nanoparticles in synthesis of 2-amino-4*H*-benzo [h] chromenes and reduction of 4-nitrophenol. J Mol Struct 1253:132102. https://doi.org/10.1016/j.molstruc.2021.132102
Rajesh UC, Purohit G, Rawat DS (2015) One-pot synthesis of aminoindolizines and chalcones using CuI/CSP nanocomposites with anomalous selectivity under green conditions. ACS Sustain Chem Eng 3:2397–2404. https://doi.org/10.1021/acssuschemeng.5b00701
Reddy GM, Garcia JR, Zyryanov GV, Sravya G, Reddy NB (2019) Pyranopyrazoles as efficient antimicrobial agents: green, one pot and multicomponent approach. Bioorg Chem 82:324–331. https://doi.org/10.1016/j.bioorg.2018.09.035
Reeves JB, McCarty GW, Rutherford DW, Wershaw RL (2007) Near infrared spectroscopic examination of charred pine wood, bark, cellulose and lignin: implications for the quantitative determination of charcoal in soils. J near Infrared Spectrosc 15:307–315. https://doi.org/10.1255/jnirs.742
Ren Y-M, Cai C (2008) Convenient and efficient method for synthesis of substituted 2-amino-2-chromenes using catalytic amount of iodine and K_2CO_3 in aqueous medium. Catal Commun 9:1017–1020. https://doi.org/10.1016/j.catcom.2007.10.002
Ro KS, Cantrell KB, Hunt PG (2010) High-temperature pyrolysis of blended animal manures for producing renewable energy and value-added biochar. Ind Eng Chem Res 49:10125–10131. https://doi.org/10.1021/ie101155m

Rousta M, Khalili D, Khalafi-Nezhad A, Ebrahimi E (2021) CuO-decorated magnetite-reduced graphene oxide: a robust and promising heterogeneous catalyst for the oxidative amidation of methylarenes in water via benzylic sp3 C–H activation. New J Chem 45:20007–20020. https://doi.org/10.1039/D1NJ03982B

Ruiz-Cornejo JC, Sebastián D, Lázaro MJ (2020) Synthesis and applications of carbon nanofibers: a review. Rev Chem Eng 36:493–511. https://doi.org/10.1515/revce-2018-0021

Sadjadi S, Heravi MM, GhoreyshiKahangi F (2019a) Salep as a biological source for the synthesis of biochar with utility for the catalysis. Appl Organometal Chem 33:e4990. https://doi.org/10.1002/aoc.4990

Sadjadi S, Heravi MM, Mohammadi L, Malmir M (2019b) Pd@magnetic carbon dot immobilized on the cyclodextrin nanosponges—biochar hybrid as an efficient hydrogenation catalyst. Chem Select 4:7300–7307. https://doi.org/10.1002/slct.201901451

Samantaray S, Pradhan D, Hota G, Mishra B (2012) Catalytic application of CeO_2–CaO nanocomposite oxide synthesized using amorphous citrate process toward the aqueous phase one pot synthesis of 2-amino-2-chromenes. Chem Eng J 193:1–9. https://doi.org/10.1016/j.cej.2012.04.011

Saravana Ganesan N, Suresh P (2020) Nitrogen-doped graphene oxide as a sustainable carbonaceous catalyst for greener synthesis: benign and solvent-free synthesis of pyranopyrazoles. ChemistrySelect 5:4988–4993. https://doi.org/10.1002/slct.202000748

Shaabani A, Maleki A (2007) Cellulose sulfuric acid as a bio-supported and recyclable solid acid catalyst for the one-pot three-component synthesis of α-amino nitriles. Appl Catal A 331:149–151. https://doi.org/10.1016/j.apcata.2007.07.021

Shaabani B, Maleki H, Rakhtshah J (2019) Environmentally benign synthesis of pyranopyrazole derivatives by cobalt Schiff-base complexes immobilized on magnetic iron oxide nanoparticles. J Organomet Chem 897:139–147. https://doi.org/10.1016/j.jorganchem.2019.06.030

Shan R, Han J, Gu J, Yuan H, Luo B, Chen Y (2020) A review of recent developments in catalytic applications of biochar-based materials. Resour Conserv Recycl 162:105036. https://doi.org/10.1016/j.resconrec.2020.105036

Sheldon RA (2007) The E factor: fifteen years on. Green Chem 9:1273–1283. https://doi.org/10.1039/B713736M

Shen Y, Fu Y (2018) Advances in in situ and ex situ tar reforming with biochar catalysts for clean energy production. Sustain Energy Fuels 2:326–344. https://doi.org/10.1039/C7SE00553A

Sikandar S, Zahoor AF (2021) Synthesis of pyrano[2,3-c]pyrazoles: a review. J Heterocycl Chem 58:685–705. https://doi.org/10.1002/jhet.4191

Singha R, Basak P, Ghosh P (2022) Catalytic applications of graphene oxide towards the synthesis of bioactive scaffolds through the formation of carbon–carbon and carbon–heteroatom bonds. Phys Sci Rev. https://doi.org/10.1515/psr-2021-0096

Solhy A, Elmakssoudi A, Tahir R, Karkouri M, Larzek M, Bousmina M, Zahouily M (2010) Clean chemical synthesis of 2-amino-chromenes in water catalyzed by nanostructured diphosphate Na_2 CaP_2O_7. Green Chem 12:2261–2267. https://doi.org/10.1039/C0GC00387E

Steingruber HS, Mendioroz P, Diez AS, Gerbino DC (2020) A green nanopalladium-supported catalyst for the microwave-assisted direct synthesis of xanthones. Synthesis 52:619–628. https://doi.org/10.1055/s-0039-1691069

Suja P, John J, Rajan T, Anilkumar GM, Yamaguchi T, Pillai SC, Hareesh U (2023) Graphitic carbon nitride (gC_3N_4) based heterogeneous single atom catalysts: synthesis, characterisation and catalytic applications. J Mater Chem A 11:8599–8646. https://doi.org/10.1039/D2TA09776A

Surpur MP, Kshirsagar S, Samant SD (2009) Exploitation of the catalytic efficacy of Mg/Al hydrotalcite for the rapid synthesis of 2-amino-chromene derivatives via a multicomponent strategy in the presence of microwaves. Tetrahedron Lett 50:719–722. https://doi.org/10.1016/j.tetlet.2008.11.114

Tang J, Zhu W, Kookana R, Katayama A (2013) Characteristics of biochar and its application in remediation of contaminated soil. J Biosci Bioeng 116:653–659. https://doi.org/10.1016/j.jbiosc.2013.05.035

Tian B, Du S, Guo F, Dong Y, Mao S, Qian L, Liu Q (2021) Synthesis of biomimetic monolithic biochar-based catalysts for catalytic decomposition of biomass pyrolysis tar. Energy 222:120002. https://doi.org/10.1016/j.energy.2021.120002

Tian B, Mao S, Guo F, Bai J, Shu R, Qian L, Liu Q (2022) Monolithic biochar-supported cobalt-based catalysts with high-activity and superior-stability for biomass tar reforming. Energy 242:122970. https://doi.org/10.1016/j.energy.2021.122970

Tian B et al (2022a) Catalytic conversion of toluene as a biomass tar model compound using monolithic biochar-based catalysts decorated with carbon nanotubes and graphic carbon covered Co-Ni alloy nanoparticles. Fuel 324:124585. https://doi.org/10.1016/j.fuel.2022.124585

Tobío-Pérez I, Domínguez YD, Machín LR, Pohl S, Lapuerta M, Piloto-Rodríguez R (2022) Biomass-based heterogeneous catalysts for biodiesel production: a comprehensive review. Int J Energy Res 46:3782–3809. https://doi.org/10.1002/er.7436

Trinkunaite-Felsen J, Stankeviciute Z, Yang JC, Yang TCK, Beganskiene A, Kareiva A (2014) Calcium hydroxyapatite/whitlockite obtained from dairy products: simple, environmentally benign and green preparation technology. Ceram Int 40:12717–12722. https://doi.org/10.1016/j.ceramint.2014.04.120

Trost BM (1995) Atom economy—a challenge for organic synthesis: homogeneous catalysis leads the way Angew. Chem Int Engl 34:259–281. https://doi.org/10.1002/anie.199502591

Veisi H, Pirhayati M, Mohammadi P, Tamoradi T, Hemmati S, Karmakar B (2023) Recent advances in the application of magnetic nanocatalysts in multicomponent reactions. RSC Adv 13:20530–20556. https://doi.org/10.1039/D3RA01208E

Velusamy K, Devanand J, Senthil Kumar P, Soundarajan K, Sivasubramanian V, Sindhu J, Vo D-VN (2021) A review on nano-catalysts and biochar-based catalysts for biofuel production. Fuel 306:121632. https://doi.org/10.1016/j.fuel.2021.121632

Vidal JL, Andrea VP, MacQuarrie SL, Kerton FM (2019) Oxidized biochar as a simple, renewable catalyst for the production of cyclic carbonates from carbon dioxide and epoxides. ChemCatChem 11:4089–4095. https://doi.org/10.1002/cctc.201900290

Vidal JL, Wyper OM, MacQuarrie SL, Kerton FM (2021) Ring-closing metathesis of aliphatic ethers and esterification of terpene alcohols catalyzed by functionalized biochar. Eur J Org Chem 2021:6052–6056. https://doi.org/10.1002/ejoc.202101256

Wang Y, Huang L, Zhang T, Wang Q (2022) Hydrogen-rich syngas production from biomass pyrolysis and catalytic reforming using biochar-based catalysts. Fuel 313:123006. https://doi.org/10.1016/j.fuel.2021.123006

Wang J, Yuan S, Dai X, Dong B (2023a) Application, mechanism and prospects of Fe-based/Fe-biochar catalysts in heterogenous ozonation process: a review. Chemosphere 319:138018. https://doi.org/10.1016/j.chemosphere.2023.138018

Wang N, Cheng L, Liao Y, Xiang Q (2023b) Effect of functional group modifications on the photocatalytic performance of g-C3N4. Small 25:2300109. https://doi.org/10.1002/smll.202300109

Wu Y et al (2021) Enhancing hydrodeoxygenation of bio-oil via bimetallic Ni-V catalysts modified by cross-surface migrated-carbon from biochar. ACS Appl Mater Interfaces 13:21482–21498. https://doi.org/10.1021/acsami.1c05350

Xie Y, Chen H, Liao J, Zhang Y (2022) Conversion of sheep manure to biochar and its U(VI) removal application: green and sustainable method to overcome manure contamination. Biomass Conv Bioref. https://doi.org/10.1007/s13399-022-03183-9

Xiong X, Yu IKM, Cao L, Tsang DCW, Zhang S, Ok YS (2017) A review of biochar-based catalysts for chemical synthesis, biofuel production, and pollution control. Bioresour Technol 246:254–270. https://doi.org/10.1016/j.biortech.2017.06.163

Xu R et al (2022) Development of metal-doping mesoporous biochar catalyst for co-valorizing biomass and plastic waste into valuable hydrocarbons, syngas, and carbons. Fuel Process Technol 227:107127. https://doi.org/10.1016/j.fuproc.2021.107127

Yang X et al (2022) Tunable syngas production from biomass: synergistic effect of steam, Ni–CaO catalyst, and biochar. Energy 254:123904. https://doi.org/10.1016/j.energy.2022.123904

Yu X, Yuan D, Mi X (2021) Hydrothermal synthesis and luminescent properties of $Ca_3(PO_4)_2$:Dy3+ white-emitting phosphors. J Alloy Compd 857:157585. https://doi.org/10.1016/j.jallcom.2020.157585

Zaimes GG, Soratana K, Harden CL, Landis AE, Khanna V (2015) Biofuels via fast pyrolysis of perennial grasses: a life cycle evaluation of energy consumption and greenhouse gas emissions. Environ Sci Technol 49:10007–10018. https://doi.org/10.1021/acs.est.5b00129

Zhang Y, Zhang L, Gao R, Zhong L, Xue J (2021) $CaCO_3$-coated PVA/BC-based composite for the simultaneous adsorption of Cu(II), Cd(II), Pb(II) in aqueous solution. Carbohyd Polym 267:118227. https://doi.org/10.1016/j.carbpol.2021.118227

Zhang F, Yang K, Liu G, Chen Y, Wang M, Li S, Li R (2022) Recent advances on graphene: synthesis, properties and applications. Compos A Appl Sci Manuf 160:107051. https://doi.org/10.1016/j.compositesa.2022.107051

Zhang S-Z, Cui Z-S, Zhang M, Zhang Z-H (2022b) Biochar based functional materials as heterogeneous catalysts for organic reactions. Curr Opin Green Sustain Chem 38:100713. https://doi.org/10.1016/j.cogsc.2022.100713